Learning Language-Conditioned Deformable Object Manipulation with Graph Dynamics

Kai Mo[†], Yuhong Deng[†], Chongkun Xia and Xueqian Wang[*]

Abstract— Vision-based deformable object manipulation is a challenging problem in robotic manipulation, requiring a robot to infer a sequence of manipulation actions leading to the desired state from solely visual observations. Most previous works address this problem in a goal-conditioned way and adapt the goal image to specify a task, which is not practical or efficient. Thus, we adapted natural language specification and proposed a language-conditioned deformable object manipulation policy learning framework. We first design a unified Transformer-based architecture to understand multi-modal data and output picking and placing action. Besides, we have introduced the visible connectivity graph to tackle non-linear dynamics and complex configuration of the deformable object in the manipulation process. Both simulated and real experiments have demonstrated that the proposed method is general and effective in language-conditioned deformable object manipulation policy learning. Our method achieves much higher success rates on various language-conditioned deformable object manipulation tasks (87.3% on average) than the state-of-the-art method in simulation experiments. Besides, our method is much lighter and has a 75.6% shorter inference time than state-of-the-art methods. We also demonstrate that our method performs well in real-world applications. Supplementary videos can be found at **https://sites.google.com/view/language-deformable**.

I. INTRODUCTION

Deformable objects are common in the application scenarios of industrial [1] and service [2] robots. Recently, vision-based deformable object manipulation has been widely investigated. The robot is supposed to infer a sequence of manipulation actions from solely visual observations to manipulate a deformable object into a prescribed goal configuration [3], [4]. Early works focus on learning task-specific manipulation skills and have limited application. Goal image specification has become a feasible solution for learning manipulation policy of more diverse tasks, where goal images specify the goal configurations [5], [6]. However, goal image specifications require much human effort to generate goal images and are complicated for non-experts.

To eliminate the limitation of goal image specification, we propose a language-conditioned deformable object manipulation learning framework, where natural language instructions are used to specify manipulation tasks. There are some studies in language-conditioned manipulation policy learning with the rapid development of LLM (large language model). In previous work, the robot only needed to

Instruction:

"fold two sleeves to the center, then fold the bottom hem to the collar."

① fold the left sleeve to the center ② fold the right sleeve to the center ③ fold the bottom hem to the collar ④ fold the bottom hem to the collar ⑤ Task completed !
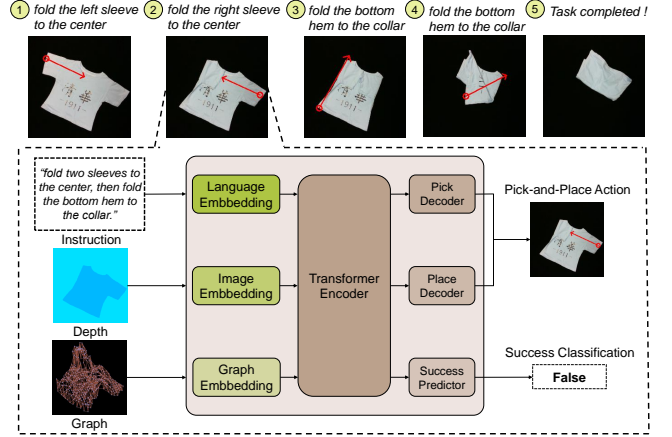
Fig. 1. **Overview**. To solve language-conditioned deformable object manipulation tasks, we design a unified Transformer-based architecture and introduce graph representation. Our solution framework performs well even on sequential multi-step deformable object manipulation tasks.

execute templated manipulations like picking, placing, and moving rigid objects [7], [8]. However, deformable object manipulation tasks are often sequential multi-step tasks. Thus, language-conditioned deformable object manipulation tasks pose higher requirements for inference and decision-making at the intersection of vision, language, and action. In addition, the manipulation planning task is also more difficult because the deformable object has nonlinear dynamics [9] and complex configurations [10].

We design a unified Transformer-based model architecture (Fig. 1) to tackle the challenge of inference and decision-making on multi-modal data. We first implement a CLIP [11] model that is pre-trained on millions of image-caption pairs from the internet, which can provide a powerful prior for grounding language in visual scenes. The natural language instruction is encoded with CLIP's Transformer-based sentence encoder to provide language embeddings. As for the image, we borrow the method in ViT [12] (Vision Transformer). We split an image into patches and get the visual embeddings by linear projection. Besides, we introduce graph embeddings to deal with deformable dynamics and configurations. We establish a visible connectivity graph [13] to represent the deformable object configurations and get the graph embeddings by linearly projecting representation vectors of graph nodes. Compared with previous graph representation methods of deformable objects [14], [15], the visible connectivity graph has two types of edges: nearby

† indicates the authors with equal contributions.

All of the authors are with the Center for Intelligent Control and Telescience, Tsinghua Shenzhen International Graduate School, Shenzhen, China {mok21, dengyh20}@mails.tsinghua.edu.cn, {xiachongkun, wang.xq}@sz.tsinghua.edu.cn

*Corresponding author: *Xueqian Wang*

edges and inferred mesh edges, which can overcome the challenges of partial observability and self-occlusions.

After obtaining the language, image, and graph embeddings, we apply position embeddings [16] in language and image embeddings. We do not apply position embeddings in graph embeddings because Transformer without position embedding is permutation-invariant and a natural fit for graphs. The language, image, and graph embeddings will then pass through the type embedding layer [17] to achieve multi-modal data fusion. Finally, all embeddings will pass through a Transformer encoder layer [18] and generate picking and placing action possibility distribution, where positions with max possibility will be picking and placing positions. The robot will execute picking and placing actions in a close loop until the task is completed.

We present both simulated and real experiments on various language-conditioned deformable object manipulation tasks to evaluate our proposed method. The results demonstrate that our method is more efficient and general for language-conditioned deformable object manipulation than the state-of-the-art framework [7]. Real-world experiments also demonstrate the sim-to-real transferability of our framework. The contributions of this work are summarized as follows:

1) We propose a novel learning framework that extends instruction-following robots' application on sequential multi-step deformable object manipulation;
2) We propose a unified Transformer-based architecture for language-conditioned deformable object manipulation policy learning, which outperforms the state-of-the-art method;
3) We conduct experiments to demonstrate that the proposed framework outperforms state-of-the-art methods and can be zero-shot transferred to the real world.

The rest of this paper is organized as follows. The related work is reviewed in Section II. Section III presents a detailed problem definition. Section IV presents details of the learning framework design. The experimental setup and results are provided in Section V. Section VI concludes this paper and discusses future works.

II. RELATED WORK

A. Learning for Deformable Object Manipulation

Learning-based methods have recently been widely used to equip the robot with advanced deformable object manipulation skills. There are two main learning-based methods: model-based methods rely on an accurate forward dynamics model, which can predict the configurations of deformable objects under a given action. The critical issue is to obtain accurate dynamics. Tuning the involved parameters of the physical model (such as mass-spring system and continuum mechanics) can improve model prediction accuracy, which is complex and expensive [1]. Learning accurate deformable dynamics from quantities of interaction data between robots and objects is a new trend [19]. However, the learned model has poor generalization on different objects and tasks.

Besides, sample-based methods like model predictive control [20] can be used to compensate for the prediction error of the forward dynamics model, which can bring a heavy computing burden. Policy-based methods learn manipulation policy directly from observation without establishing a forward dynamics model. The robot learns manipulation policy from expert demonstrations [21] or exploratory robot interactions [22]. However, most previous policy-based methods are limited to learning task-specific policy and fail to reuse information efficiently for different tasks, which is inefficient in real-world applications [23]. To provide a general framework for deformable object manipulation, some approaches learn a goal-conditioned policy, where the robot is provided with goal images of objects [5], [6]. Unlike previous work, we adapt language instruction to specify different deformable manipulation tasks and achieve a general deformable object manipulation policy learning framework.

B. Language-conditioned Robotic Manipulation policy

Language-conditioned robotic manipulation has received growing attention recently, where the manipulation task is specified by language instruction [24], [25]. Language instruction specification is much easier to obtain than goal image specification and can specify more diversified tasks. Despite the abundant benefits of commanding robots with natural language, such agents require deep integration of multiple data modalities (language, vision, action). Language-Conditioned Imitation Learning addresses this problem by mapping actions directly from vision and language understanding in an end-to-end fashion [7]. However, collecting demonstrations paired with language annotations in the real robot is costly and time-consuming. To tackle this data-collecting problem, Nair et al. [26] adopt crowd-sourced annotation to obtain sufficient datasets. Although some works improve the model's performance in more diverse languages [27], [28], previous language-conditioned robotic manipulation approaches are limited in manipulation objects. The robot only needs to manipulate a rigid object with low-level skills such as grasping and pushing. Simplifying objects and actions will limit the application scenarios because deformable object manipulation skills are essential in many human-robot interaction tasks. Thus, we propose a solution framework that can be applied to complex deformable object manipulation tasks.

III. PROBLEM FORMULATION

Our goal is to learn a language-conditioned deformable object manipulation policy $\pi_{\boldsymbol{\theta}}$ parameterized by $\boldsymbol{\theta}$, which can generate a sequence of manipulation action $\{\boldsymbol{a}_t\}(t = 0, 1, 2, ...T)$ in a closed-loop manner from a natural language instruction $\mathbf{s}$ and the current visual observation $\mathbf{o}_t$:

$$\boldsymbol{a}_t \leftarrow \pi_{\boldsymbol{\theta}}(\mathbf{o}_t, \mathbf{s})$$
$$\text{and} \quad \mathbf{o}_{t+1} \leftarrow \mathcal{T}(\mathbf{o}_t, \boldsymbol{a}_t) \tag{1}$$

where $\mathcal{T}$ denotes the state transition describing the deformable dynamics. Since the deformable object has a complex configuration, the visual observation $\mathbf{o}$ is composed of
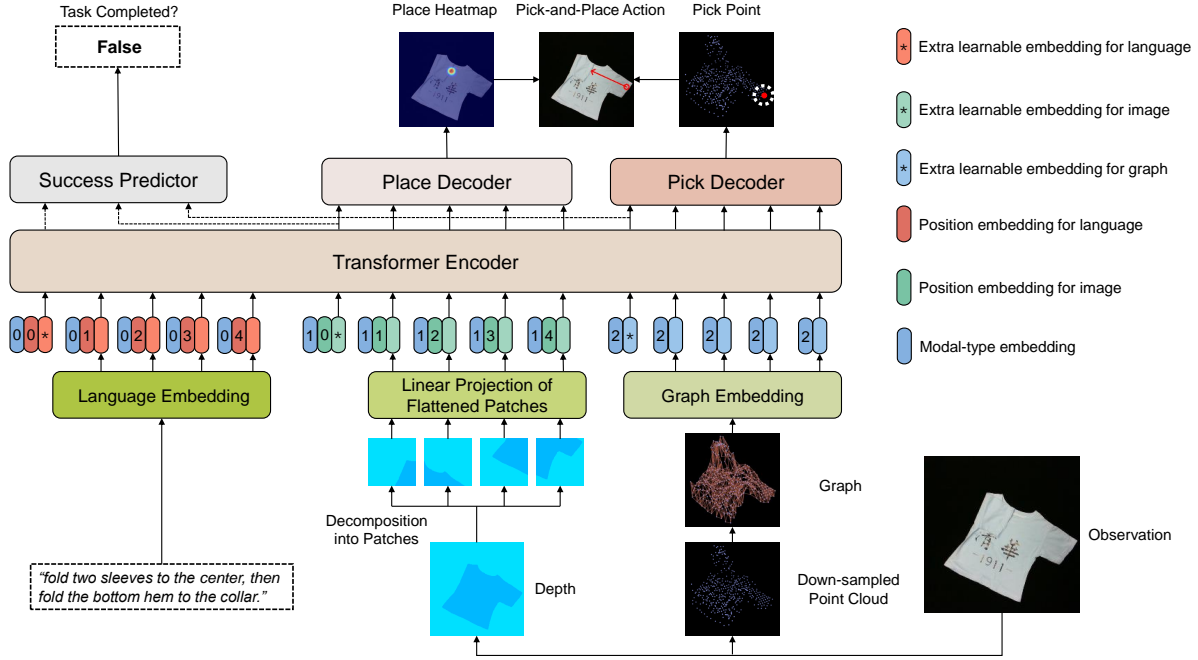
Fig. 2. **Method overview.** We design a unified Transformer-based architecture to understand the multi-modal data and output pick-and-place action with task completion prediction. To tackle the challenge of the deformable objects' partial observability and complex dynamics, we introduce a visible connectivity graph representation to pose the inductive bias of the deformable objects' physics to the framework.

two parts in our solution framework: the top-down depth image $\mathbf{I}$ and the representation graph $\mathbf{G}(\mathbf{P})$ established from the point cloud $\mathbf{P}$:

$$\boldsymbol{a}_t \leftarrow \pi_{\boldsymbol{\theta}}(\mathbf{I}_t, \mathbf{G}(\mathbf{P}_t), \mathbf{s}) \qquad (2)$$

The action space is defined as picking and placing action:

$$\boldsymbol{a}_t = \{\boldsymbol{a}_t^{\text{pick}}, \boldsymbol{a}_t^{\text{place}}\} \qquad (3)$$

where $\boldsymbol{a}_t^{\text{pick}}$ and $\boldsymbol{a}_t^{\text{place}}$ denote the robot end-effector's poses while picking and placing part of the object respectively.

We formulate the problem of language-conditioned deformable object manipulation as a supervised learning problem. The policy $\pi_{\boldsymbol{\theta}}$ is learned from a data set of expert demonstrations.

IV. LEARNING FOR LANGUAGE-CONDITIONED DEFORMABLE OBJECT MANIPULATION

This section presents details of our learning framework for language-Conditioned deformable object manipulation. Fig. 2 shows the overview of the architecture.

A. Multi-modal data embedding

The framework takes as input a language instruction, a depth image, and a graph. We first leverage different modules to embed these multi-modal data.

Language Embedding: We use a pre-trained language model to embed the language instruction $\mathbf{s}$. Specifically, we employ the language encoder in the CLIP model [11], providing a powerful prior for grounding language in visual scenes. Similar to prior works [12], [29], we prepend an extra learnable embedding for aggregating the language representation and add learnable position embeddings to

retain positional information. Mathematically, the language embedding z_s is computed as follows:

$$z_s = [S_{head}; \text{CLIP}(\mathbf{s})] + S_{pos} \qquad (4)$$

where $\text{CLIP}()$ denotes the CLIP's language encoder that produces a sequence of tokens whose dimension is always $\mathbb{R}^{77 \times 512}$ (with zero-padding), $S_{head} \in \mathbb{R}^{512}$ denotes the extra learnable embedding, $S_{pos} \in \mathbb{R}^{78 \times 512}$ denotes the learnable position embeddings.

Image Embedding: Inspired by the prior work [30], we use depth rather than RGB to make our framework able to be transferred to the real world without any additional training or domain randomization. We first decompose the depth image $\mathbf{I} \in \mathbb{R}^{H \times W \times 1}$ into N non-overlapping patches, each of size $B \times B$, i.e., $N = HW/B^2$. We then flatten these 2D patches into 1D vectors $x_I \in \mathbb{R}^{N \times B^2}$. We linearly map these vectors into embedding vectors of dimension $\mathbb{R}^{512}$ to align the CLIP output's dimension. We prepend an extra learnable embedding to aggregate the image representation and add learnable position embeddings for retaining positional information. Mathematically, The image embedding z_I is computed as follows:

$$z_I = [I_{head}; W_I x_I^1; W_I x_I^2; \cdots, W_I x_I^N] + I_{pos} \qquad (5)$$

where $W_I \in \mathbb{R}^{512 \times P^2}$ denotes a learnable matrix, $I_{head} \in \mathbb{R}^{512}$ denotes the extra learnable embedding, $I_{pos} \in \mathbb{R}^{(N+1) \times 512}$ denotes the learnable position embeddings.

Graph Embedding: Following the prior work [13], we introduce a visible connectivity graph $\langle V, E \rangle$ to pose the inductive bias of the deformable objects' physics to the framework. The nodes V represent the particles that compose the deformable object. The two types of edges E are nearby

edges E^C and mesh edges E^M that model the dynamics collision and the deformable object's structure, respectively. In the implementation, we apply a voxel grid filter and the farthest point sampling method to down-sample the raw point cloud observation into K points. The down-sampled point cloud $\mathbf{P} = \{v_i\}_{i=1,\cdots,K}$ constructs the nodes of the graph. We construct the nearby edges E^C based on the euclidean distance of two nodes:

$$E^C = \{e_{ij} | \|v_i - v_j\|_2 < R\} \quad (6)$$

where R is a distance threshold, and v_i, v_j are the positions of the nodes i, j. After obtaining the nearby edges E^C based on Eqn. 6, we use the pre-trained edge GNN proposed in the prior work [13] to predict the mesh edges E^M implicitly. Specifically, we input the graph $\langle \mathbf{P}, E^C \rangle$ into the pre-trained edge GNN and take out only the node embeddings until the penultimate layer since the node embeddings can aggregate some information about the edge prediction through the GNN's message passing. We also prepend an extra learnable embedding that can aggregate the graph representation. We do not add position embeddings because Transformer without position embeddings is permutation-invariant and a natural fit for graphs [16]. Mathematically, The graph embedding z_G is computed as follows:

$$z_G = [G_{head}; G_{edge}(\langle \mathbf{P}, E^C \rangle)] \quad (7)$$

where $G_{head} \in \mathbb{R}^{512}$ denotes the extra learnable embedding, $G_{edge}()$ denotes the pre-trained edge GNN in the prior work [13].

B. Encoder-decoder for Pick-and-Place

Encoder: After obtaining the embeddings corresponding to the different modal types, We make an aggregation by concatenating these multi-modal embeddings and adding modal-type embeddings:

$$z_0 = [z_s + S_{type}; z_I + I_{type}; z_G + G_{type}] \quad (8)$$

where $S_{type}, I_{type}, G_{type} \in \mathbb{R}^{512}$ are modal-type embeddings corrsponding to the language, the image and the graph, respectively.

We input the vector z_0 to a Transformer encoder with L layers proposed in ViT [12]:

$$\begin{aligned} z'_l &= \mathrm{MSA}(\mathrm{LN}(z_{l-1})) + z_{l-1} & l = 1, \cdots, L \\ z_l &= \mathrm{MLP}(\mathrm{LN}(z'_l)) + z'_l & l = 1, \cdots, L \end{aligned} \quad (9)$$

where $\mathrm{MSA}()$ denotes multiheaded self-attention, $\mathrm{LN}()$ denotes LayerNorm, and $\mathrm{MLP}()$ denotes an MLP layer.

Pick Decoder and Place Decoder: We build a pick decoder and a place decoder to predict picking and place points, respectively. The pick decoder is an MLP that contains one layer. Like Foldsformer [30], the place decoder consists of convolutional layers and upsampling operations alternately. The pick decoder takes the graph's node embeddings in the encoder output as input and outputs the probability $Q_{\mathrm{pick}} \in \mathbb{R}^K$ of each point being a pick point in the down-sampled point cloud $\mathbf{P}$. The place encoder takes the image's

patch embeddings in the encoder output as input and outputs a pixel-wise heatmap $Q_{\mathrm{place}} \in \mathbb{R}^{H \times W}$ that predicts the probability of each pixel being a place point in the image. The optimal picking point $\boldsymbol{a}_{\mathrm{pick}}$ and the optimal placing point $\boldsymbol{a}_{\mathrm{place}}$ are computed as follows:

$$\begin{aligned} \boldsymbol{a}_{\mathrm{pick}} &= \mathrm{argmax}_{\boldsymbol{a}} Q_{\mathrm{pick}}(\boldsymbol{a}) \\ \boldsymbol{a}_{\mathrm{place}} &= \mathrm{argmax}_{\boldsymbol{a}} Q_{\mathrm{place}}(\boldsymbol{a}) \end{aligned} \quad (10)$$

Success Classifier: Previous works [7], [25], [27] can not estimate whether a task has been completed. Instead, they keep taking actions until an oracle indicates the task completion and stops the execution, which is not practical in real-world employment. Thus, we design a successful classifier to estimate task completion, making our framework more autonomous. The success classifier is an MLP that contains two layers. In the encoder output, we use vectors corresponding to the three extra embeddings described in Sec. IV-A. The success classifier takes the concatenation of these embeddings and performs binary classification indicating task completion.

C. Implementation Details

Data Collection: The training data is collected in the Soft-Gym suite [31], a particle-based simulator built on Nvidia Flex. The 3D models of the T-shirt and the shorts are sampled from CLOTH3D dataset [32]. Our training data include 15 tasks (Fig. 5) with 1000 expert demonstrations per task. In SoftGym, the deformable objects are modeled as particles whose ground truth positions and velocities can be accessed. Thus, we can easily collect expert demonstrations using a scripted demonstrator. The object's initial configurations (size, pose, etc.) are randomized during data collection. Each expert demonstration ζ are composed of the language instruction $\mathbf{s}$, the observation-action pair $(\mathbf{o}_t, \boldsymbol{a}_t)$ with $t = 1, 2, \cdots, T$:

$$\zeta = \{l, (\mathbf{o}_1, \boldsymbol{a}_1), (\mathbf{o}_2, \boldsymbol{a}_2), \cdots, (\mathbf{o}_T, \boldsymbol{a}_T)\} \quad (11)$$

Training Details: We use behavioral cloning to train a multi-task model. We train the success classifier and other modules separately. We first freeze the CLIP encoder and the edge GNN and then train the modules except for the classifier with the binary cross-entropy (BCE) loss between the predicted $Q_{\mathrm{pick}}, Q_{\mathrm{place}}$ and the ground truth $Q_{\mathrm{pick}}^{gt}, Q_{\mathrm{place}}^{gt}$:

$$\mathcal{L}_{\mathrm{action}} = \mathrm{BCE}(\boldsymbol{Q}_{\mathrm{pick}}, \boldsymbol{Q}_{\mathrm{pick}}^{\mathrm{gt}}) + \mathrm{BCE}(\boldsymbol{Q}_{\mathrm{place}}, \boldsymbol{Q}_{\mathrm{place}}^{\mathrm{gt}}) \quad (12)$$

Finally, We freeze the trained modules and train the success classifier with the BCE loss.

In this work, The depth image size $(H \times W)$, the patch size (B), the number of points (K), the distance threshold (R), the layers of the Transformer encoder (L) are set to be $224 \times 224, 16, 200, 0.045, 8$, respectively. The framework is trained with a batch size of 48, a learning rate of 0.0001, and an Adam optimizer [33] for 100 epochs. It takes about 16 hours on an NVIDIA RTX 3090 GPU.

Method	towel-inward		towel-triangle		towel-double -triangle		towel-adjacent -corners-inward		towel-opposite -corners-inward	
	100	1000	100	1000	100	1000	100	1000	100	1000
Foldsformer [30]	83.3	90.0	70.0	80.0	33.3	56.7	73.3	96.7	86.7	83.3
CLIPORT [7]	83.3	86.7	80.0	83.3	70.0	73.3	73.3	80.0	76.7	83.3
ours (w/o graph)	96.7	96.7	93.3	96.7	53.3	63.3	**100.0**	**100.0**	**100.0**	**100.0**
ours (full method)	**100.0**	**100.0**	**96.7**	**100.0**	**73.3**	**76.7**	**100.0**	**100.0**	**100.0**	**100.0**
	towel-half -folding		towel-half- double-folding		towel-all- corners-inward		Tshirt-left- sleeve-inward		Tshirt-right- sleeve-inward	
	100	1000	100	1000	100	1000	100	1000	100	1000
Foldsformer [30]	30.0	46.7	3.3	6.7	80.0	93.3	33.3	36.7	26.7	30.0
CLIPORT [7]	60.0	70.0	30.0	20.0	80.0	90.0	56.7	96.7	73.3	93.3
ours (w/o graph)	63.3	76.7	**36.7**	40.0	96.7	**100.0**	96.7	**100.0**	93.3	**100.0**
ours (full method)	**73.3**	**86.7**	30.0	**53.3**	**100.0**	**100.0**	**100.0**	**100.0**	**100.0**	**100.0**
	Tshirt-two- sleeves-inward		Tshirt-half -folding		Tshirt-folding		shorts-half -folding		shorts-folding	
	100	1000	100	1000	100	1000	100	1000	100	1000
Foldsformer [30]	13.3	30.0	13.3	13.3	0.0	6.7	16.7	30.0	0.0	10.0
CLIPORT [7]	**100.0**	**100.0**	43.3	46.7	0.0	30.0	50.0	73.3	0.0	20.0
ours (w/o graph)	83.3	93.3	50.0	70.0	20.0	50.0	70.0	83.3	6.7	23.3
ours (full method)	96.7	**100.0**	**66.7**	**83.3**	**33.3**	**63.3**	**96.7**	**100.0**	**16.7**	**46.7**

V. EXPERIMENTS

This section presents simulated and real-world experiments to answer the following questions: 1) How well does our framework compare with the baseline methods on language-conditioned deformable object manipulation tasks? 2) What role does the visible connectivity graph play in our algorithm design? and 3) How well does our framework perform on real-world language-conditioned deformable object manipulation tasks?

A. Simulation Experiments

We first compare the performance of our method with baseline methods in simulation. Specifically, in each experiment of language-conditioned deformable object manipulation task, the robot is provided with a natural language instruction and is supposed to complete the instruction with only current visual observation inputs.

Baseline Methods:

1) Foldsformer [30] is a state-of-the-art method that adapts a sequence of sub-goal images to specify the task. It can complete similar tasks on clothes of different configurations with a general demonstration. Foldsformer is provided with a fixed set of sub-goals rather than a natural language instruction in each task.
2) CLIPORT [7] represents the typical network for language-conditioned manipulation learning. It relies on a two-stream architecture and uses pre-trained vision-language models for precise manipulation policies with language goals.

3) Ours (w/o graph) has the same backbone architecture as the proposed algorithm. The only difference is that we did not provide it with graph information, and the model needs to infer language-conditioned policy from the depth image and natural language instruction.

Success Rate: We compare the above methods' success rates of completing unseen language-conditioned deformable manipulation tasks. The success metric is the mean particle position error between the cloth states achieved by the policy and a scripted demonstrator that can access the ground truth particle positions. Specifically, we define a task as a success if the mean particle position error is less than 0.0125 m (the diameter of a particle in SoftGym) and otherwise as a failure. We evaluate the success rate on 15 types of language-conditioned tasks (each type of task has 30 unseen task instances) and train all models with 100 and 1000 demonstrations separately.

The results are shown in TABLE I. Overall, Foldsformer performs worst, illustrating the merits of natural language specification in creating a general agent of robotic manipulation. Compared with a demonstration of an image sequence, natural language can provide sufficient cues of task requirements without over-defining the task by the object's texture, position, and size. Besides, a demonstration could only capture one instance of success [34]. All of these factors have limited the generality of learned policy and explain why Foldsformer did not perform as well as the other three types of model that adopt nature language instruction.

Ours (w/o graph) generally outperforms CLIPORT, demonstrating that the proposed model architecture effec-
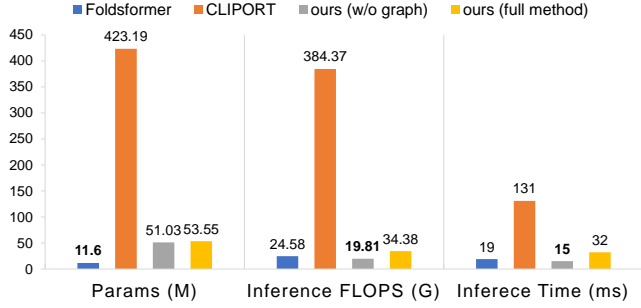
Fig. 3. **Model Capacity.** We compare our model's model parameters, FLOPs, and inference time with those of baseline models.

tively teaches language-conditioned manipulation policy. We adopt CLIP to get language embeddings and borrow Vit to get visual embeddings. Finally, Transformer-based architecture is used to output picking and placing action from multi-modal embedding fused by model-type embedding. Such model architecture performs well in learning language-conditioned manipulation policy and outperforms the state-of-the-art method.

By introducing a visible connectivity graph, ours (full method) outperforms all baseline methods. Particularly on tasks with more steps and complex deformable objects (such as T-shirt and shorts-folding), our method shows more significant advantages of achieving higher success rates than the baseline models. These tasks are more complicated, where the manipulation process is more likely to cause irregular self-occlusion and partial observation. These results demonstrate that the visible connectivity graph can help the robot to capture the deformable dynamics and configurations more accurately in some complex scenarios.

In addition, our method also achieves much higher sample efficiency than baseline methods. In TABLE I, the success rates of our model trained on 100 demonstrations are much higher than those of baseline models trained on 100 demonstrations or even 1000 demonstrations on almost all involved tasks. These results demonstrate that compared with other models, our model is more effective in learning language-conditioned deformable object manipulation policy.

Model Capacity: Besides superior performance on language-conditioned deformable object manipulation, our model is much lighter and simpler than the baseline methods. For a detailed comparison, we calculate the FLOPs (Floating Point Operations), model parameters, and inference times of our model and baseline models. We run the analysis on a machine with an NVIDIA GeForce RTX 3090 GPU and an Intel Xeon W-2223 CPU (3.6GHz).

The results are shown in Fig. 3. Overall, Foldsformer is the lightest model among these models because Foldsfomer infers manipulation policies from only images without dealing with multi-modal data. Among three types of language-conditioned manipulation policy learning models, ours (full method) and ours (w/o graph) are dramatically (more than one order of magnitude) lighter in model FLOPs and parameters than CLIPORT, which also leads to much
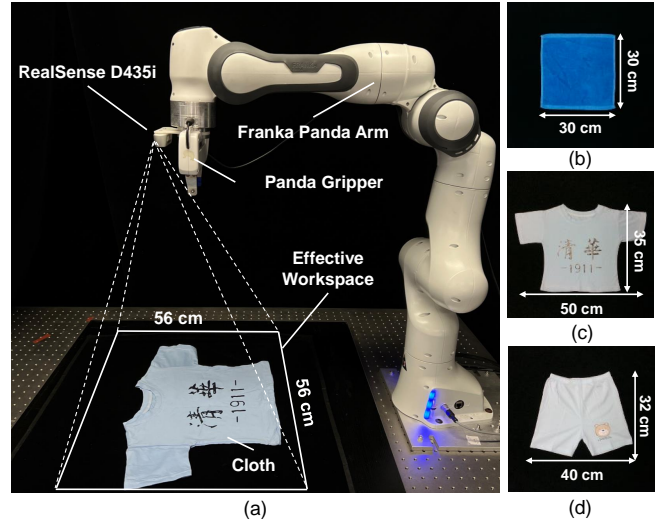

Fig. 4. **Experimental Setup.** (a) Robot system. (b) A 30 cm × 30 cm cloth. (b) A 50 cm × 35 cm T-shirt. (c) A pair of shorts (40 cm $times$ 32 cm).

less (almost five times) inference time. The proposed model architecture does not rely on complex convolution operations adapted in CLIPORT. We design a unified transformer-based architecture to tackle the intersection of vision, language, and action, significantly improving the model's efficiency. Besides, introducing graph representation does not significantly increase FLOPs (Floating Point Operations), model parameters, and inference times. Improving model performance by introducing graph representation is feasible in terms of model efficiency.

B. Real World Experiments

As described previously, we use depth images rather than RGB images to make our framework able to be transferred to the real world without any additional training or domain randomization. We evaluate the sim-to-real performance of our framework with a 7-DOF Franka Emika Panda robot arm with a standard two-finger panda gripper (Fig. 4). A Realsense RGB-D camera fixed on the platform's top captures visual observations. We crop the RGB-D image into the size of 480×480, corresponding to a workspace of $56cm \times 56cm$. The deformable object is placed on the platform in front of the robot. We use a $30cm \times 30cm$ towel, a $50cm \times 35cm$ T-shirt, and a pair of shorts ($40cm \times 32cm$) in the experiments. Similar to previous works [4], [6], [30], we quantitatively evaluate the performance by two metrics: Mean Intersection over Union (MIoU) between the cloth masks achieved by our framework and a human demonstrator; A penalty for wrinkles (WR), which calculates the percentage of pixels inside the cloth mask detected as edges by the Canny edge detector.

Table. II shows the quantitative results. The average value of MIoU is close to 1, and the average value of mean WR is close to 0, demonstrating that our model performs close to human experts on real-world language-conditioned deformable object manipulation tasks. Fig. 5 shows some
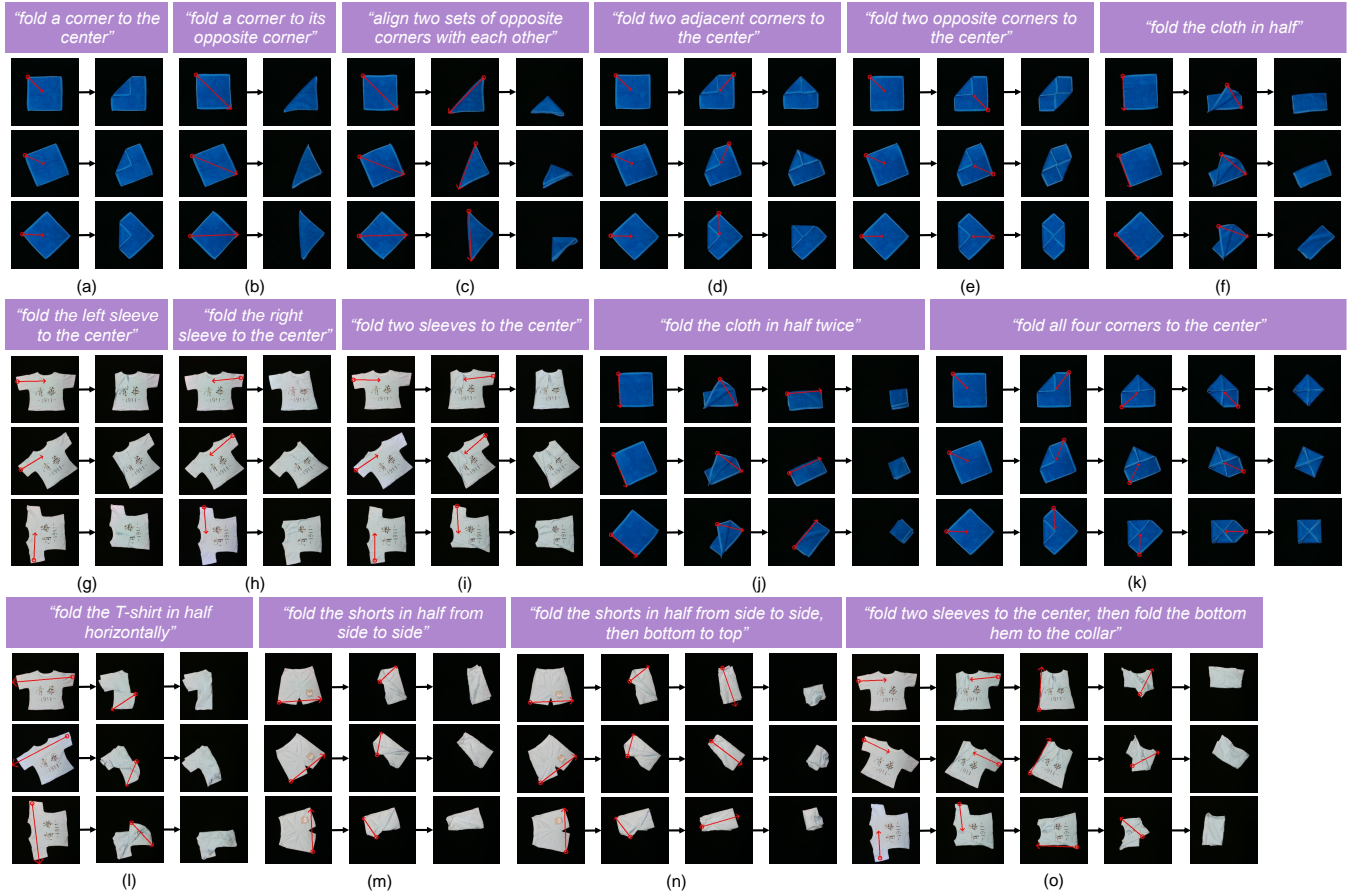
Fig. 5. **Qualitative Results in Real World Experiments.** Our framework performs 15 tasks in the real world: (a) towel-inward. (b) towel-triangle. (c) towel-double-triangle. (d) towel-adjacent-corners-inward. (e) towel-opposite-corners-inward. (f) towel-half-folding. (g) Tshirt-left-sleeve-inward. (h) Tshirt-right-sleeve-inward. (i) Tshirt-two-sleeves-inward. (j) towel-double-half-folding. (k) towel-all-corners-inward. (l) Tshirt-half-folding. (m) shorts-half-folding. (n) shorts-folding. (o) Tshirt-folding. Pick-and-place actions are visualized as red arrows.

examples in our real experiments. For each type of task, we provide three instances. Our model completes all involved real tasks specified by language instruction. At each timestep, we show the selected optimal pick and place actions. A full video recording of these experiments can be found on our project website.

VI. CONCLUSION

In this paper, we propose a novel framework for language-conditioned deformable manipulation policy learning. A unified Transformer-based architecture is designed to deal with multi-modal data and output precise picking and placing action. To solve self-occlusion and partial observation, we construct a visible connective graph to understand the spatial structure of the deformable object. Extensive experiments have been conducted to verify the proposed model architecture's performance, proving that the visible connective graph can help the robot capture complex deformable configurations. Furthermore, our framework can also generalize to real scenarios. Our method has paved the way for advanced language-conditioned manipulation skills learning (even sequential multi-step deformable object manipulation). For future work, we will explore language diversity with some LLMs (large language models) on the proposed framework.

TABLE II

REAL EXPERIMENT RESULTS. AVERAGE MIOU AND MEAN WR ON 15 LANGUAGE-CONDITIONED DEFORMABLE OBJECT MANIPULATION TASKS IN THE REAL WORLD.

Task	MIoU	mean WR
towel-inward	0.988	0.017
towel-triangle	0.861	0.027
towel-double-triangle	0.923	0.045
towel-adjacent-corners-inward	0.962	0.026
towel-opposite-corners-inward	0.957	0.027
towel-half-folding	0.896	0.030
towel-double-half-folding	0.847	0.042
towel-all-corners-inward	0.910	0.051
Tshirt-left-sleeve-inward	0.966	0.037
Tshirt-right-sleeve-inward	0.962	0.034
Tshirt-two-sleeves-inward	0.917	0.046
Tshirt-half-folding	0.842	0.038
Tshirt-folding	0.833	0.024
shorts-half-folding	0.912	0.050
shorts-folding	0.825	0.073

REFERENCES

[1] H. Yin, A. Varava, and D. Kragic, "Modeling, learning, perception, and control methods for deformable object manipulation," *Science Robotics*, vol. 6, no. 54, p. eabd8803, 2021.

[2] B. Thananjeyan, A. Garg, S. Krishnan, C. Chen, L. Miller, and K. Goldberg, "Multilateral surgical pattern cutting in 2d orthotropic gauze with deep reinforcement learning policies for tensioning," in

2017 IEEE international conference on robotics and automation (ICRA), pp. 2371–2378, IEEE, 2017.

[3] B. Thach, B. Y. Cho, A. Kuntz, and T. Hermans, "learning visual shape control of novel 3d deformable objects from partial-view point clouds," in *2022 International Conference on Robotics and Automation (ICRA)*, pp. 8274–8281, IEEE, 2022.

[4] T. Weng, S. M. Bajracharya, Y. Wang, K. Agrawal, and D. Held, "Fabricflownet: Bimanual cloth manipulation with a flow-based policy," in *Conference on Robot Learning*, pp. 192–202, PMLR, 2022.

[5] D. Seita, P. Florence, J. Tompson, E. Coumans, V. Sindhwani, K. Goldberg, and A. Zeng, "Learning to rearrange deformable cables, fabrics, and bags with goal-conditioned transporter networks," in *2021 IEEE International Conference on Robotics and Automation (ICRA)*, pp. 4568–4575, IEEE, 2021.

[6] R. Lee, D. Ward, V. Dasagi, A. Cosgun, J. Leitner, and P. Corke, "Learning arbitrary-goal fabric folding with one hour of real robot experience," in *Conference on Robot Learning*, pp. 2317–2327, PMLR, 2021.

[7] M. Shridhar, L. Manuelli, and D. Fox, "Cliport: What and where pathways for robotic manipulation," in *Conference on Robot Learning*, pp. 894–906, PMLR, 2022.

[8] A. Brohan, Y. Chebotar, C. Finn, K. Hausman, A. Herzog, D. Ho, J. Ibarz, A. Irpan, E. Jang, R. Julian, *et al.*, "Do as i can, not as i say: Grounding language in robotic affordances," in *6th Annual Conference on Robot Learning*, 2022.

[9] S. Zimmermann, R. Poranne, and S. Coros, "Dynamic manipulation of deformable objects with implicit integration," *IEEE Robotics and Automation Letters*, vol. 6, no. 2, pp. 4209–4216, 2021.

[10] J. Zhu, A. Cherubini, C. Dune, D. Navarro-Alarcon, F. Alambeigi, D. Berenson, F. Ficuciello, K. Harada, J. Kober, X. Li, *et al.*, "Challenges and outlook in robotic manipulation of deformable objects," *IEEE Robotics & Automation Magazine*, vol. 29, no. 3, pp. 67–77, 2022.

[11] A. Radford, J. W. Kim, C. Hallacy, A. Ramesh, G. Goh, S. Agarwal, G. Sastry, A. Askell, P. Mishkin, J. Clark, *et al.*, "Learning transferable visual models from natural language supervision," in *International conference on machine learning*, pp. 8748–8763, PMLR, 2021.

[12] A. Dosovitskiy, L. Beyer, A. Kolesnikov, D. Weissenborn, X. Zhai, T. Unterthiner, M. Dehghani, M. Minderer, G. Heigold, S. Gelly, *et al.*, "An image is worth 16x16 words: Transformers for image recognition at scale," *arXiv preprint arXiv:2010.11929*, 2020.

[13] X. Lin, Y. Wang, Z. Huang, and D. Held, "Learning visible connectivity dynamics for cloth smoothing," in *Conference on Robot Learning*, pp. 256–266, PMLR, 2022.

[14] Y. Deng, C. Xia, X. Wang, and L. Chen, "Deep reinforcement learning based on local gnn for goal-conditioned deformable object rearranging," in *2022 IEEE/RSJ International Conference on Intelligent Robots and Systems (IROS)*, IEEE, 2022.

[15] C. Wang, Y. Zhang, X. Zhang, Z. Wu, X. Zhu, S. Jin, T. Tang, and M. Tomizuka, "Offline-online learning of deformation model for cable manipulation with graph neural networks," *IEEE Robotics and Automation Letters*, vol. 7, no. 2, pp. 5544–5551, 2022.

[16] Z. Wu, P. Jain, M. Wright, A. Mirhoseini, J. E. Gonzalez, and I. Stoica, "Representing long-range context for graph neural networks with global attention," *Advances in Neural Information Processing Systems*, vol. 34, pp. 13266–13279, 2021.

[17] W. Kim, B. Son, and I. Kim, "Vilt: Vision-and-language transformer without convolution or region supervision," in *International Conference on Machine Learning*, pp. 5583–5594, PMLR, 2021.

[18] A. Vaswani, N. Shazeer, N. Parmar, J. Uszkoreit, L. Jones, A. N. Gomez, Ł. Kaiser, and I. Polosukhin, "Attention is all you need," *Advances in neural information processing systems*, vol. 30, 2017.

[19] W. Yan, A. Vangipuram, P. Abbeel, and L. Pinto, "Learning predictive representations for deformable objects using contrastive estimation," in *Conference on Robot Learning*, pp. 564–574, PMLR, 2021.

[20] X. Ma, D. Hsu, and W. S. Lee, "Learning latent graph dynamics for visual manipulation of deformable objects," in *2022 International Conference on Robotics and Automation (ICRA)*, pp. 8266–8273, IEEE, 2022.

[21] A. Nair, D. Chen, P. Agrawal, P. Isola, P. Abbeel, J. Malik, and S. Levine, "Combining self-supervised learning and imitation for vision-based rope manipulation," in *2017 IEEE international conference on robotics and automation (ICRA)*, pp. 2146–2153, IEEE, 2017.

[22] J. Matas, S. James, and A. J. Davison, "Sim-to-real reinforcement learning for deformable object manipulation," in *Conference on Robot Learning*, pp. 734–743, PMLR, 2018.

[23] Y. Wu, W. Yan, T. Kurutach, L. Pinto, and P. Abbeel, "Learning to manipulate deformable objects without demonstrations," in *Robotics: Science and Systems*, 2020.

[24] E. Stengel-Eskin, A. Hundt, Z. He, A. Murali, N. Gopalan, M. Gombolay, and G. Hager, "Guiding multi-step rearrangement tasks with natural language instructions," in *Conference on Robot Learning*, pp. 1486–1501, PMLR, 2022.

[25] M. Shridhar, L. Manuelli, and D. Fox, "Perceiver-actor: A multi-task transformer for robotic manipulation," *arXiv preprint arXiv:2209.05451*, 2022.

[26] S. Nair, E. Mitchell, K. Chen, S. Savarese, C. Finn, *et al.*, "Learning language-conditioned robot behavior from offline data and crowdsourced annotation," in *Conference on Robot Learning*, pp. 1303–1315, PMLR, 2022.

[27] P.-L. Guhur, S. Chen, R. Garcia, M. Tapaswi, I. Laptev, and C. Schmid, "Instruction-driven history-aware policies for robotic manipulations," *arXiv preprint arXiv:2209.04899*, 2022.

[28] O. Mees, L. Hermann, E. Rosete-Beas, and W. Burgard, "Calvin: A benchmark for language-conditioned policy learning for long-horizon robot manipulation tasks," *IEEE Robotics and Automation Letters*, 2022.

[29] W. Kim, B. Son, and I. Kim, "Vilt: Vision-and-language transformer without convolution or region supervision," in *International Conference on Machine Learning*, pp. 5583–5594, PMLR, 2021.

[30] K. Mo, C. Xia, X. Wang, Y. Deng, X. Gao, and B. Liang, "Foldsformer: Learning sequential multi-step cloth manipulation with space-time attention," *IEEE Robotics and Automation Letters*, vol. 8, no. 2, pp. 760–767, 2023.

[31] X. Lin, Y. Wang, J. Olkin, and D. Held, "Softgym: Benchmarking deep reinforcement learning for deformable object manipulation," in *Conference on Robot Learning*, pp. 432–448, PMLR, 2021.

[32] H. Bertiche, M. Madadi, and S. Escalera, "Cloth3d: clothed 3d humans," in *Computer Vision–ECCV 2020: 16th European Conference, Glasgow, UK, August 23–28, 2020, Proceedings, Part XX 16*, pp. 344–359, Springer, 2020.

[33] D. P. Kingma and J. Ba, "Adam: A method for stochastic optimization," *arXiv preprint arXiv:1412.6980*, 2014.

[34] S. Nair, E. Mitchell, K. Chen, S. Savarese, C. Finn, *et al.*, "Learning language-conditioned robot behavior from offline data and crowdsourced annotation," in *Conference on Robot Learning*, pp. 1303–1315, PMLR, 2022.